Abstract

Measurement of the positive kaon-argon total hadronic differential cross section in the LArIAT experiment

Elena Gramellini

2018

Abstract goes here. Limit 750 words.

Measurement of the positive kaon-argon total hadronic differential cross section in the LArIAT experiment

A Dissertation
Presented to the Faculty of the Graduate School
of
Yale University
in Candidacy for the Degree of
Doctor of Philosophy

by
Elena Gramellini

Dissertation Director: Bonnie T. Fleming

Date you'll receive your degree

Contents

List of Figures

List of Tables

Acknowledgements

A lot of people are awesome. But not you, who are reading my thesis before it's done.

Chapter 1

Introduction

1.1 The Standard Model

The Standard Model (SM) of particle physics the most accurate theoretical description of the subatomic world and, more generically, one of the most precisely tested theories in the history of physics. The SM describes the strong, electromagnetic and weak interactions among elementary particles in the framework of quantum field theory, accounting for the unification of electromagnetic and weak interactions for energies above the vacuum expectation value of the Higgs field. The SM does not describe gravity or general relativity.

The Standard Model is a gauge theory based on the local group of symmetry

$$G_{SM} = SU(3)_C \otimes SU(2)_T \otimes U(1)_Y \tag{1.1}$$

where the subscripts indicate the conserved charges: the strong charge, or color C, the weak isospin T (or rather its third component T3) and the hypercharge Y. These quantities can be related to the electric charge Q through the Gell-Mann-Nishijima relation:

$$Q = \frac{Y}{2} + T_3. \tag{1.2}$$

Generation	I	II	III	T	Y	Q
Leptons	$\begin{pmatrix} \nu_e \\ e \end{pmatrix}_L$	$\begin{pmatrix} \nu_\mu \\ \mu \end{pmatrix}_L$	$\begin{pmatrix} \nu_\tau \\ \tau \end{pmatrix}_L$	$1/2$ $-1/2$	-1 -1	0 -1
	e_R	μ_R	τ_R	0	-2	1
Quarks	$\begin{pmatrix} u \\ d' \end{pmatrix}_L$	$\begin{pmatrix} c \\ s' \end{pmatrix}_L$	$\begin{pmatrix} t \\ b' \end{pmatrix}_L$	$1/2$ $-1/2$	$1/3$ $1/3$	$2/3$ $-1/3$
	u_R d'_R	c_R s'_R	t_R b'_R	0 0	$4/3$ $-2/3$	$2/3$ $-1/3$

Table 1.1: SM elementary fermions. The subscripts L and R indicate respectively the negative helicity (left-handed) and the positive helicity (right-handed).

In the quantum field framework, the elementary particles correspond to the irreducible representations of the G_{SM} symmetry group. In particular, the particles are divided in two categories, fermions and bosons, according to their spin-statistics. Described by the Fermi-Dirac statistics, Fermions have half-integer spin and are sometimes called "matter-particles". Bosons or "force carriers" have integer spin, follow the Bose-Einstein statistics and mediate the interaction between fermions. The fundamental fermions and their quantum numbers are listed in Tab 1.1.

Quarks can interact via all three the fundamental forces; they are triplets of $SU(3)_C$, that is they can exist in three different colors: C = R, G, B. If one chooses a base where u, c and t quarks are simultaneously eigenstates of both the strong and the weak interactions, the remaining eigenstates are usually written as d, s and b for the strong interaction and d', s' and b' for the weak interaction, because the latter ones are the result of a Cabibbo rotation on the first ones. Charged leptons interact via the weak and the electromagnetic forces, while neutrinos only interact via the weak force. The gauge group univocally determines the number of gauge bosons that carry the interaction; the gauge bosons correspond to the generators of

the group: eight gluons (g) for the strong interaction, one photon (γ) and three bosons ($W^{\pm}$, Z^0) for the electroweak interaction. A gauge theory by itself can not provide a description of massive particles, but it is experimentally well know that most of the elementary particles have non-zero masses. The introduction of massive fields in the Standard Model lagrangian would make the theory non-renormalizable, and - so far - mathematically impossible to handle. This problem is solved in the Standard Model by the introduction of a scalar iso-doublet $\Phi(x)$, the Higgs field, which gives mass to $W^{\pm}$ and Z^0 gauge bosons through the electroweak symmetry breaking and to the fermions through Yukawa coupling [1, 2].

1.2 Neutrinos: in and beyond the Standard Model

1.2.1 Neutrino in the SM

Neutrino were introduced in the SM as left-handed massless Weyl spinors. The Dirac equation of motion

$$(i\gamma^{\mu}\partial_{\mu} - m)\psi = 0 \tag{1.3}$$

for a fermionic field

$$\psi = \psi_L + \psi_R \tag{1.4}$$

is equivalent to the equaitons

$$i\gamma^{\mu}\partial_{\mu}\psi_L = m\psi_R \tag{1.5}$$

$$i\gamma^{\mu}\partial_{\mu}\psi_R = m\psi_L \tag{1.6}$$

for the chiral fields ψ_R and ψ_L, whose evolution in space and time is coupled through the mass m. If the fermion is massless, the chiral fields decouple and the fermion can be described by a single Weyl spinor with two independent components. Pauli initially rejected the description of a physical particle through a single Wyle

spinor because of its implication of parity violation. In fact, since the spatial inversion operator throws $\psi_R \leftrightarrow \psi_L$, parity is conserved only if the both the chiral components exist at the same time. ADD CITATIONS. For the neutrino introduction in the SM, experiments came in help of the theoretical description: the constraint of parity conservation weakened after Wu's experiment ADD CITATIONS AND DATES, there was no experimental indication for massive neutrinos and neutrinos likely interacted only via the left-handed component.

The symmetry group $SU(2)_T \otimes U(1)_Y$ is the only group relevant for neutrino interactions. The SM electroweak lagrangian is the most general renormalizable lagrangian invariant under the local symmetry group $SU(2)_T \otimes U(1)_Y$. The lagrangian couples the weak isotopic spin doublets and singlets described in 1.1 with the gauge bosons A^μ_a (a = 1,2,3) and B^μ, and Higgs doublet $\Phi(x)$:

$$
\begin{aligned}
\mathcal{L} = & \, i \sum_{\alpha=e,\mu,\tau} \bar{L}'_{\alpha L} \not{D} L'_{\alpha L} + i \sum_{\alpha=1,2,3} \bar{Q}'_{\alpha L} \not{D} Q'_{\alpha L} \\
& + i \sum_{\alpha=e,\mu,\tau} \bar{l}'_{\alpha R} \not{D} l'_{\alpha R} + i \sum_{\alpha=d,s,b} \bar{q}'^{D}_{\alpha R} \not{D} q'^{D}_{\alpha R} + i \sum_{\alpha=u,c,t} \bar{q}'^{U}_{\alpha R} \not{D} q'^{U}_{\alpha R} \\
& - \frac{1}{4} A_{\mu\nu} A^{\mu\nu} - \frac{1}{4} B_{\mu\nu} B^{\mu\nu} \\
& + (D_\rho \Phi)^\dagger (D^\rho \Phi) - \mu^2 \Phi^\dagger \Phi - \lambda (\Phi^\dagger \Phi)^2 \\
& - \sum_{\alpha,\beta=e,\mu,\tau} \left(Y'^{l}_{\alpha\beta} \bar{L}'_{\alpha L} \Phi l'_{\beta R} + Y'^{l*}_{\alpha\beta} \bar{l}'_{\beta R} \Phi^\dagger L'_{\alpha L} \right) \\
& - \sum_{\alpha=1,2,3} \sum_{\beta=d,s,b} \left(Y'^{D}_{\alpha\beta} \bar{Q}'_{\alpha L} \Phi q'^{D}_{\beta R} + Y'^{D*}_{\alpha\beta} \bar{q}'^{D}_{\beta R} \Phi^\dagger Q'_{\alpha L} \right) \\
& - \sum_{\alpha=1,2,3} \sum_{\beta=u,c,t} \left(Y'^{U}_{\alpha\beta} \bar{Q}'_{\alpha L} \widetilde{\Phi} q'^{U}_{\beta R} + Y'^{U*}_{\alpha\beta} \bar{q}'^{U}_{\beta R} \widetilde{\Phi}^\dagger Q'_{\alpha L} \right).
\end{aligned} \tag{1.7}
$$

The first two lines of the lagrangian summarize the kinetic terms for the fermionic fields and their coupling to the gauge bosons $A^{\mu\nu}_a$, $B^{\mu\nu}$ [1]. The third line describes

1. In gauge theories the ordinary derivative ∂_μ is substitued with the covariant derivative D_μ. Here $D_\mu = \partial_\mu + igA_\mu \cdot I + ig' B_\mu \frac{Y}{2}$, where I and Y are the $SU(2)_L$ and $U(1)_Y$ generators, respectively.

the kinetic terms and the self-coupling terms of the gauge bosons. The forth line is the Higgs lagrangian, which results in the spontaneous symmetry breaking. The last three lines describe the Yukawa coupling between fermions and the Higgs field, origin of the fermion's mass.

The coupling between left-handed and right-handed field generates the mass term for fermions. The SM assumes only left-handed components for neutrinos, thus implying zero neutrino mass. Since any linear combination of massless fields results in a massless field, the flavor eigenstates are identical to the mass eigenstates in the SM.

1.2.2 Neutrino Oscillations

The determination of the flavor of a neutrino dynamically arises from the corresponding charged lepton associated in a CC interaction; for example, a ν_e is a neutrino which produces an e^-, a $\bar{\nu}_\mu$ is a neutrino which produces a μ^+, *etc.* The neutrino flavor eigenstates $|\nu_\alpha\rangle$, with $\alpha = e, \mu, \tau$, are orthogonal to each other and form a base for the the weak interaction matrix.

Overwhelming experimental data show neutrinos change flavor during their propagation. This phenomenon, predicted by Bruno Pontecorvo in 1957, is called "neutrino oscillations" and it is possible only if the flavor eigenstate are not identical to the mass eigenstates. A minimal extension of the Standard Model introduces three mass eigenstates, $|\nu_i\rangle$ $(i = 1, 2, 3)$, whose mass m_i is well defined. The unitary Pontecorvo-Maki-Nakagawa-Sakata matrix transforms the spinor wave functions (ψ) of each component between flavor and mass bases as follows

$$\sum \psi_\alpha |\nu_\alpha\rangle = \sum \psi_i |\nu_i\rangle, \rightarrow \psi_\alpha = U_{PMNS}\psi_i, \tag{1.8}$$

with

$$U_{PMNS} = \begin{bmatrix} c_{12} & s_{12} & 0 \\ -s_{12} & c_{12} & 0 \\ 0 & 0 & 1 \end{bmatrix} \begin{bmatrix} c_{13} & 0 & s_{13}e^{-i\delta} \\ 0 & 1 & 0 \\ -s_{13}e^{-i\delta} & 0 & c_{13} \end{bmatrix} \begin{bmatrix} 1 & 0 & 0 \\ 0 & c_{23} & s_{23} \\ 0 & -s_{23} & c_{23} \end{bmatrix} \begin{bmatrix} e^{i\alpha_1} & 0 & 0 \\ 0 & e^{i\alpha_2} & 0 \\ 0 & 0 & 1 \end{bmatrix} \tag{1.9}$$

where c e s stand respectively for cosine and sine of the corresponding mixing angles (θ_{12}, θ_{23} and θ_{13}), δ is the Dirac CP violation phase, α_1 and α_2 is the eventual Majorana CP violation phases.

Experimental results summary

1.3 Beyond the Standard Model

The discovery of neutrino oscillation and its implication of non-zero neutrino mass mark the beginning of a new, exciting era in neutrino physics: the era of physics Beyond the Standard Model (BSM) in the neutrino sector. We are currently searching for new, deeper theories that can accommodate neutrinos with non-zero mass, while remaining consistent with the rest of the Standard Model.

Open Questions in Neutrino Physics

On one hand, the last X decades of experiments in neutrino oscillations brought spectacular advancements in the understanding of the oscillations pattern, measuring the neutrino mixing angles and mass splitting with a precision of less than 10%. On the other, it opened the field for a series of questions needing experimental answers. Critical challenges in the next decade will entail an even deeper understanding of the neutrino mixing pattern, investigation of the neutrino mass origin, neutrino number and nature, and assessing CP violation in the lepton sector.

Following the recommendation of the latest Particle Physics Project Prioritization

Panel [3], the US is dedicating substantial resources to the development of a short- and long- baseline neutrino program to address many of these fundamental questions. This program pivots on the Liquid Argon Time Projection Chamber (LArTPC) detector technology which will be described in 2.

The main goals of these research programs include:

- Assessment of the existence of right-handed sterile neutrinos.

- Determination of the sign of Δm^2_{13} (or Δm^2_{23}), i.e., the "neutrino mass ordering".

- Determination of the octant, i.e. whether θ_{23} is maximal.

- Determination the status of CP symmetry in the lepton sector.

Smallness of neutrino masses, link to GUTs

Towards a more fundamental theory

Despite its highly predictive power, a number of conceptual issues arise in the SM which disfavor it to be a good candidate for a fundamental theory.

The SM rather complex group structure, where a gauge group is formed with the direct product of other three groups as shown in eq. 1.1, is unexplained. Also, the SM fails to include a suitable dark matter candidate and a mechanisms that accounts for the baryon asymmetry of the universe. Within the SM, a total of 25 parameters remain seemingly arbitrary and need to be fitted to data: 3 gauge couplings, 9 charged fermion masses, 3 mixing angles and one CP phase in the CKM matrix, the Higgs mass and quartic coupling, θ_{QCD}, 3 neutrino masses, 3 neutrino mixing angles, 1 Dirac phase and, eventually, 2 Majorana phases.

Chapter 2

Liquid Argon Detectors at the Intensity Frontier

In the next few years, LArTPC experiments – such as the Short-Baseline Neutrino program (SBN) and DUNE – will be major players in the intensity frontier field.

2.1 The SBN Program

2.1.1 SBN Goals

2.1.2 Neutrino Interactions and Detection

2.2 DUNE

2.2.1 DUNE Non-Accelerator Physics Program

2.2.2 Rare Decay Searches: Experimental Limit

2.2.3 Nucleon Decay Detection in LAr

2.3 Liquid Argon Time Projection Chambers at the Intensity Frontier

2.3.1 Time Projection Chamber

2.3.2 Ionization Detectors with Noble Liquids

2.3.3 LArTPC: Principles of Operation

2.3.4 Liquid Argon Ionization Charge Detection

Electron Life Time & purity

Space Charge Effect

Recombination Effect

2.3.5 Liquid Argon scintillation Light Detection

LAr Scintillation Process

Wavelength Shifting of LAr Scintillation Light

Chapter 3

LArIAT: Liquid Argon In A Testbeam

3.1 LArIAT & the Intensity Frontier

3.2 Testbeam and Beamline Detectors

3.3 In the Cryostat

3.3.1 TPC: Charge Collection

3.3.2 TPC: Light Collection System

3.3.3 Cryogenics and Purity Control

3.3.4 TPC: Electric Field Measurement

3.4 Trigger and DAQ

3.5 Control Systems

Chapter 4

Kaon Interactions in Argon

Your first chapter is probably an introduction. But who knows.

Chapter 5

Data Collection

Your first chapter is probably an introduction. But who knows.

Chapter 6

LArIAT Monte Carlo

6.1 Beamline

6.1.1 G4Beamline

6.1.2 Data Driven MC

6.2 TPC MC

Chapter 7

Energy Calibration

Your first chapter is probably an introduction. But who knows.

Chapter 8

Tracking Optimization

Understanding how kaons and pions are tracked inside the TPC and optimizing the reconstruction algorithms to maximize the correct identification of the interaction point is a fundamental step of the analysis.

8.1 MC sample and WC2TPC match

The optimization is performed on a MC sample of HOW MANY? kaons and 359000 pions produced with the DDMC technique. DDMC particles are shot from the WC4 location into the TPC following the beam profile. We mimic the matching between the WC and the TPC track on Monte Carlo by constructing a fake WC track using truth information at wire chamber four. We then apply the same WC to TPC matching algorithm as in data.

Plots I want in this section:

1. WC2TPC MC DeltaX, DeltaY and α
2. Delta L, reco - true
3. Delta L, reco - true Elastic, Delta L, reco - true Inelastic, other

4. Length Quality cut

5. Efficiency as a function of true KE and Angle

8.2 Wire chamber-to-TPC match

8.2.1 Wire chamber-to-TPC match: importance and definition

something something about why this match is important

In data, we attempt to uniquely match one WC-Track to one and only one reconstructed TPC track. This match is done by using in the X and Y coordinate of the extrapolated WC-Track to the upstream most point of the reconstructed TPC Track and by using the angle between the incoming track angle and the reconstructed TPC. We define ΔX as the difference between the x position of the most upstream point of the TPC track and the x position of the WC track as projected to the TPC front face. ΔY is defined analogously. We define ΔR as $\Delta \mathrm{R} = \sqrt{\Delta \mathrm{X}^2 + \Delta \mathrm{Y}^2}$. The angle between the incident WC Track and the TPC track in the plane that contains them defines α.

We define a match between WC-track and TPC reconstructed track if $\Delta \mathrm{R} < r_T$, $\alpha < \alpha_T$ and the Z position of the first reconstructed point of the TPC track is within 2 cm from the TPC front face. The determination of the best r_T and α_T is the scope of the following section.

In MC, we mimic the matching between the WC and the TPC track on Monte Carlo by constructing a fake WC track using truth information at wire chamber four. We then apply the same WC to TPC matching algorithm as in data.

8.2.2 Matching optimization

Scope of this optimization study is assessing the goodness of the wire chamber-to-TPC match on Monte Carlo and porting the optimized selection cuts to data. A word of caution is necessary here. With this study, we want to minimize pathologies associated with the presence of the primary kaon itself, like the incorrect association between the beamline kaon its decay products inside the TPC. Assessing the contamination from pile-up[1], albeit related, is beyond the scope of this study .

In MC, we are able to define a correct WC2TPC match using the Geant4 truth information. We are thus able to count how many times the WC tracks get associated incorrectly with the wrong TPC reconstructed track.

We define a correct match if the all following conditions are met:

- the length of the true primary Geant4 track in the TPC is greater than 2 cm,
- the length of the reconstructed track length is greater than 2 cm,
- the Z position of the first reconstructed point is within 2 cm from the TPC front face
- the distance between the reconstructed track and the true entering point is the minimum compared with all the other reconstructed tracks.

In order to count the wrong matches, we consider all the reconstructed tracks whose Z position of the first reconstructed point lies within 2 cm from the TPC front face. Events with true length in TPC ¡ 2 cm included. Since kaons are shot 100 cm upstream from the TPC front face, the following two scenarios are possible from a truth standpoint:

$[Ta\ ]$ the primary kaon decays or interact strongly before getting to the TPC,

1. We remind the reader that the DDMC is a single particle Monte Carlo, where the beam pile up is not simulated.

[Tb] the primary kaon enters the TPC.

Once we choose the selection cuts to determine a reconstructed wire chamber-to-TPC match, the following four scenarios are possible :

1) no reconstructed tracks are matched

2) the correct track and one (or more) wrong tracks are matched

3) only the correct track is matched

4) one (or more) wrong track is matched.

If we keep only events with one and only one match, we discard cases 1) and 2) from the cross section measurement. For each set of α and ΔR selection value, we define purity and efficiency of the selection as follows:

$$\text{Efficiency} = \frac{\text{events with correct track matched}}{\text{events with primary in TPC}} \tag{8.1}$$

$$\text{Purity} = \frac{\text{Events with correct track matched}}{\text{Events with correct track matched + Events with wrong track matched}} \tag{8.2}$$

Chapter 9

Kaon Cross Section Measurement

Your first chapter is probably an introduction. But who knows.

Appendix A

Measurement of LArIAT Electric Field

Appendix B

Construction of A Cosmic Ray Tagger for MicroBooNE

Appendix C

Pion Analysis

C.0.1 Data Sample

We decided to use only the data from the -60 A, -100 A RunII configurations, because the beam composition for these 2 beamline configurations is available in G4Beamline. Run II data is better than Run I in terms of calorimetry and understanding of the detector.

The used SamWeb definition is PionAna_RunII_60A_100A_lovely1_elenag_00 =

Defined as "defname: Lovely1 and data_tier digits and lariat_mid_f_mc7anb ¡ 0 and create_date ¡ '2017-06-02' and run_number != 9276 and run_number != 9277 and run_number != 8836 and run_number != 9083 and run_number != 9122 and run_number != 8977 and run_number != 8981 and run_number != 8982 and run_number != 8983 and run_number != 8984 and run_number != 8985 and run_number != 8991 and run_number != 8994 and run_number != 8996 and run_number ¿= 8767 and run_number ¡= 9635"

C.0.2 Capture and Decay

Our goal is to measure the total hadronic cross section for negative pions in argon. Since pion capture can be classified as an electromagnetic process and pion decay is

Table C.1: My caption

Stage	-100A +64 GeV	-60A +64 GeV	Number of Evt
SamWebDefinition	32.7%	67.3%	3569206
WCQuality	37.8%	63.2%	553486
$P_{WC4} > 420$ MeV/c	50.8%	49.2%	423294
TOF Cut	32.7%	67.3%	

a week process, capture and decay represent unwanted interactions in our sample. We present here a study of capture and decay in Monte Carlo and the solution we adopted to mitigate their present in our sample.

For this MC study, we use a sample of 359000 MC pions generated according to the beam profile with the DDMC described in 6.1.2. Unlike decay – which may occur both in flight and at rest – capture occurs predominantly at rest. Thus, we can highly mitigate capture and decay at rest by removing pions whose energy is low enough to stop in the TPC. This translates into a momentum selection, where we keep only events whose WC momentum is above a certain threshold. Figure C.1 shows the true momentum distribution for the primary[1] pions that arrive to the TPC (pink), that capture (green) or decay (blue) inside the TPC, on a linear and log scale vertical axis.

In order to choose the selection value for the wire chamber momentum, it is beneficial to estimate the ratio of events which capture or decay that survive the selection in MC as a function of the momentum threshold, and compare it with the survival ratio for all events. This is done in figure C.2. We define the survival ratio simply as the number of events surviving the true momentum cut divided by the number of events of that given category. The survival ratio calculated separately for the three event categories explained above: total (pink), capture (green) and decay (blue). Selecting pions with momentum greater than 420 MeV/c reduces the capture

1. We use here the Geant4 denomination "primary" to indicate that the pion considered does not undergo interactions modifying its energy before getting to the TPC. In fact, not every pion shot from wire chamber four will arrive to the TPC as primary, some will decay or interact before the TPC, as explained in reference to WC 2 TPC chapter

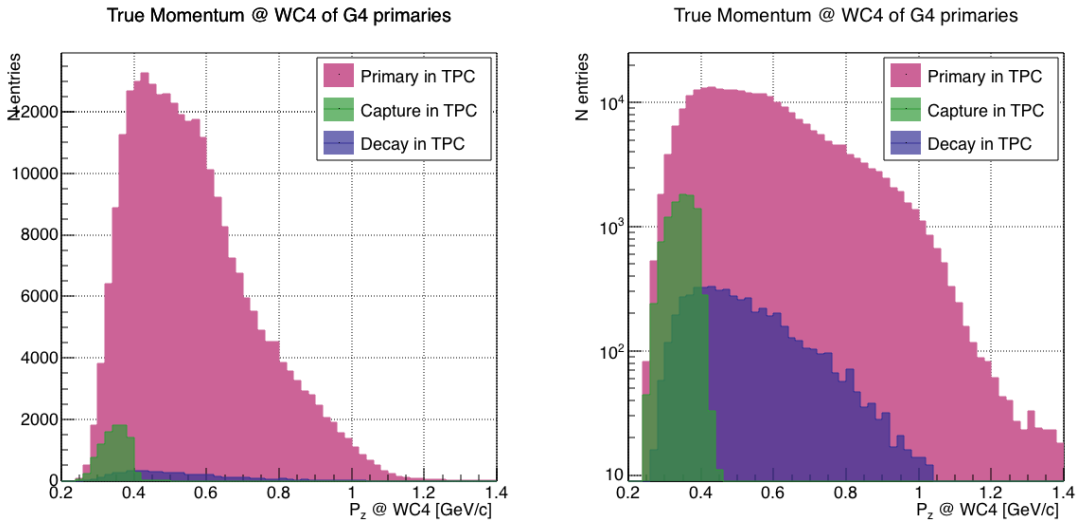

Figure C.1: True momentum distribution at wire chamber 4 for every simulated pion arriving in the TPC (pink), ending its life in capture (green) or in decay (blue) in the TPC, linear vertical axis on the left, logarithmic on the right.

events by 99% while maintaining about 80% of the total data sample. Figure C.3 shows the ratio of events which end their life in capture (green) or decay (blue) over the total number of events as a as a function of the true momentum at wire chamber four. This ratio is slightly dependent on the inelastic cross section implemented in Geant4, as we are able to register a pion capture (or decay) only if it doesn't interact inelastically in the TPC. For momenta greater than 420 MeV/c, the percentage of capture events drops below 1% and the percentage of decays is never above 2%.

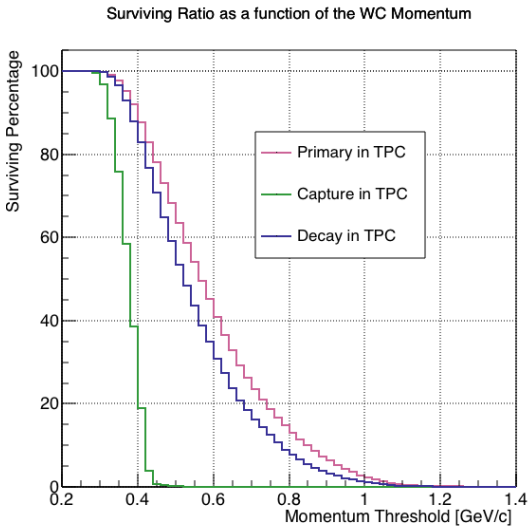

Figure C.2: Survival ratio as a function of selection threshold on true momentum at wire chamber four for for every simulated pion arriving in the TPC (pink), capture (green) or in decay (blue).

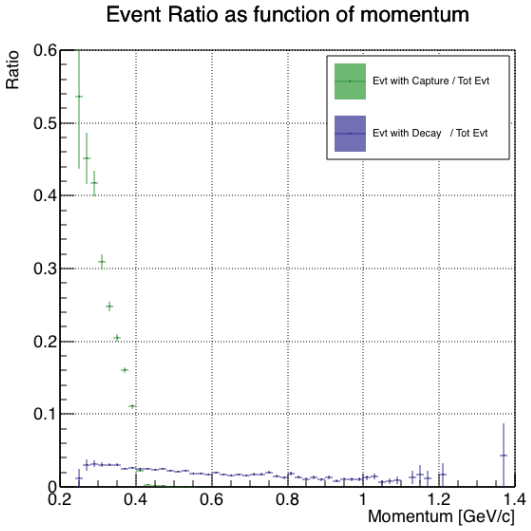

Figure C.3: Ratio between the capture (green) and decay (blue) events over the total number of events as a as a function of the true momentum at wire chamber four.

Bibliography

[1] Peter W. Higgs. Broken symmetries and the masses of gauge bosons. *Physical Review Letters*, 13(16):508–509, oct 1964.

[2] P.W. Higgs. Broken symmetries, massless particles and gauge fields. *Physics Letters*, 12(2):132–133, sep 1964.

[3] Steve Ritz et al. Building for Discovery: Strategic Plan for U.S. Particle Physics in the Global Context. 2014.